Mon. Not. R. Astron. Soc. **000**, 1–10 (2011) Printed 6 April 2014 (MN LATEX style file v2.2)

New Method for Exploring Super-Eddington AGNs by Near-infrared Observations

N. Kawakatu[1] ⋆ and K. Ohsuga [2]
[1] *Graduate School of Pure and Applied Sciences, University of Tsukuba, 1-1-1 Tennodai, Tsukuba 305-8571*
[2] *National Astronomical Observatory of Japan, 2-21-1 Osawa, Mitaka, Tokyo 181-8588, Japan*

ABSTRACT
We propose a new method to explore the candidate super-Eddington active galactic nuclei (AGNs). We examine the properties of infrared (IR) emission from the inner edge of the dusty torus in AGNs, which are powered by super- or sub-Eddington accretion flows around black holes, by considering the dependence of the polar angle on the radiation flux of accretion flows (Watarai et al. 2005). We find that for super-Eddington AGNs, of which the mass accretion rate is more than 10^2 times larger than the Eddington rate, the ratio of the AGN IR luminosity and the disc bolometric luminosity is less than 10^{-2}, unless the half opening angle of the torus ($\theta_{\rm torus}$) is small ($\theta_{\rm torus} < 65^\circ$). This is due to the self-occultation effect, whereby the self-absorption at the outer region of the super-Eddington flow dilutes the illumination of the torus. Such a small luminosity ratio is not observed in sub-Eddington AGNs, whose mass accretion rate is comparable to or no more than 10 times larger than the Eddington mass accretion rate, except for extremely thin tori ($\theta_{\rm torus} > 85^\circ$). We also consider the properties of the near-IR (NIR) emission radiated from hot dust > 1000 K. We find that super-Eddington AGNs have a ratio of the NIR luminosity to the bolometric luminosity, $L_{\rm NIR,AGN}/L_{\rm bol,disc}$, at least one order of magnitude smaller than for sub-Eddington AGNs for a wide range of half opening angle ($\theta_{\rm torus} > 65^\circ$), for various types of dusty torus model. Thus, a relatively low $L_{\rm NIR,AGN}/L_{\rm bol,disc}$ is a property that allows identification of candidate super-Eddington AGNs. Lastly, we discuss the possibility that NIR-faint quasars at redshift $z \sim 6$ discovered by a recent deep SDSS survey may be young quasars whose black holes grow via super-Eddington accretion.

Key words: accretion: accretion disc—black hole physics— galaxies:active

1 INTRODUCTION

It is now widely accepted that most normal galaxies have central supermassive black holes (SMBHs) with $M_{\rm BH} = 10^{6-9} M_\odot$ (e.g.,Kormendy & Richiston 1995; Miyoshi et al. 1995; Gillessen et al. 2009). High resolution observations of nearby galaxies have revealed a close correlation between the mass of SMBHs and the bulge mass, or the velocity dispersion of the bulge (e.g., Kormendy & Richiston 1995; Ferrarese & Merritt 2000; Marconi & Hunt 2003; Häring & Rix 2004). This implies that the formation of SMBHs is strongly coupled with the formation of galaxies. However, the formation and evolution of SMBHs is still an open question and a hot topic in astrophysics.

The discovery of luminous quasars at redshift $z > 6$ shows that SMBHs of the order of billions of solar masses exist at the end of the re-ionization epoch (e.g., Fan et al. 2001, 2006; Goto 2006; Willott et al. 2007, 2010). Considering Eddington-limited accretion, $z > 6$ quasars may not form readily. Unless the seed black hole mass is large, gas accretion with low radiative efficiency and/or BH mergers significantly contribute to the growth of SMBHs (see Shapiro 2005). If super-Eddington accretion is possible, the growth timescale of BHs can be much shorter than the Eddington timescale (e.g., Kawaguchi et al. 2004; Ohsuga et al. 2005). Thus, super-Eddington accretion might explain the formation of SMBHs. Recently, Kawakatu & Wada (2009) predicted that super-Eddington accretion is required for the formation of $z > 6$ quasars with $M_{\rm BH} \approx 10^9 M_\odot$, because the final BH mass is greatly suppressed by star formation in a circumnuclear disc and AGN outflow based on the co-evolution model of SMBH growth and a circumnuclear disc (Kawakatu & Wada 2008; see also Volonteri & Rees 2005).

The occurrence of super-Eddington accretion flow has not yet been accurately verified, although this issue has been investigated since the 1970s (e.g., Shakura & Syunyaev 1973; Begelman 1978;

⋆ E-mail:kawakatu@ccs.tsukuba.ac.jp (NK)

Abramowicz et al. 1988; Houck & Chevalie 1991; Watarai & Fukue 1999; Watarai, Fukue, & Takeuchi 2000. By using two-dimensional radiation hydrodynamic simulations, Ohsuga et al. (2005) demonstrated for the fist time that quasi-steady super-Eddington disc accretion is possible, because both the radiation field and the mass accretion flow around a BH are non-spherical and the large number of photons generated in the disc is swallowed by the BH without being radiated away due to photon-trapping (see Ohsuga & Mineshige 2007). This conclusion has recently been confirmed by two-dimensional radiation magnetohydrodynamic simulations (Ohsuga et al. 2009). However, it is still unclear whether super-Eddington accretion can significantly contribute to the formation of SMBHs, because the radiation pressure and/or disc wind associated with super-Eddington accretion might play an important role in the gas accretion process in host galaxies (e.g., Silk & Rees 1998; Fabian 1999; King 2003; Ohsuga 2007).

In the local Universe, we have discovered a class of AGNs with a higher Eddington ratio among the AGN population, i.e., Narrow Line Seyfert 1 galaxies (NLS1s). They have characteristic properties such as narrow Balmer lines (e.g., Osterbrock & Pogge 1985; Pogge 2000), strong soft X-ray excess (e.g., Pounds, Done, & Osborne 1995; Boller et al. 1996, 2003) and rapid variability (e.g., Otani, Kii, & Miya 1996; Leighly 1999; Boller et al. 2002; Gallo et al. 2004). These properties indicate that they have a small black hole mass and high Eddington ratio (e.g., Brandt & Boller 1998; Hayashida 2000; Mineshige et al. 2000). The observed bolometric luminosity of NLS1s saturates at a few times the Eddington luminosity (e.g., Collin & Kawaguchi 2004; Collin et al. 2006; Mushotzky et al. 2008; Lamastra et al. 2009), which is consistent with predictions of the super-Eddington accretion disc (e.g., Watarai, Fukue, & Takeuchi 2000; Ohsuga et al. 2005, 2009). In addition, the star formation rate of NLS1 hosts is higher than that of BLS1s (Sani et al. 2010). Thus, NLS1s may be the early phase of rapid BH growth via super-Eddington accretion (e.g., Mathur 2000; Kawaguchi et al. 2004). In the high-z universe, we may speculate that super-Eddington AGNs are a more dominant population of AGNs because the lifetime of SMBH growth is closer to the cosmic age if the formation of SMBHs is mainly a gas accretion process. To confirm this, it is important to determine whether the fraction of super-Eddington AGNs increases with redshift. Some observations to date have indicated that the average Eddington ratio increases slightly with redshift (e.g., Kollmeier et al. 2006; Shen et al. 2008; Willott et al. 2010). However, we have not observed super-Eddington AGNs among high-z quasars (e.g., McLure & Dunlop 2004; Shen et al. 2008) and AGNs in high-z massive galaxies (e.g., Yamada et al. 2009). Thus, it is essential to find candidate super-Eddington AGNs before starting detailed observations.

According to unification models of AGNs, the accretion disc is surrounded by a dusty structure (e.g., Antonucci 1993; Elitzur 2008). A significant fraction of the emitted ultraviolet and optical radiation of the accretion disc is absorbed by the dust and is re-emitted at IR wavelengths. In particular, the hot dust is directly heated by the central engine and produces near-IR (NIR) emission (e.g., Rieke 1978; Haas et al. 2003). Since it has been reported that the polar angle dependence of the radiation flux for super-Eddington accretion flow deviates from that for sub-Eddington flow (e.g., Fukue 2000; Ohsuga et al. 2005; Watarai et al. 2005 hereafter W05), the reprocessed IR emission may be useful for exploring candidates of super-Eddington accretion flow in AGNs. In this paper, we investigate the properties of IR (as well as NIR) emission from the inner edge of the dusty torus, employing radiative flux from the disc accretion flows by W05, in which the radiation fluxes of sub- and super-Eddington accretion discs are given as functions of the polar angle and the mass accretion rate.

2 RADIATION FLUX FROM ACCRETION DISC

We briefly summarize the relation between the radiation flux from the accretion disc and the mass accretion rate into an SMBH. For a small mass accretion rate, i.e., $\dot{m}_{\rm BH} \equiv \dot{M}_{\rm BH}/(L_{\rm Edd}/c^2) = 1$–$10$, where $\dot{M}_{\rm BH}$ and $L_{\rm Edd}$ are the mass accretion rate into an SMBH and the Eddington luminosity, respectively, if the accretion disc is geometrically thin, it is known as a standard disc (Shakura & Syunyaev 1973). As the mass accretion rate increases ($\dot{m}_{\rm BH} \geqslant 10$), the disc becomes geometrically thick via strong radiation pressure, i.e., a slim disc, as first introduced by Abramowicz et al. (1988). The maximum thickness of the disc is about 45° because the ratio of the scale height and the disc size is approximately unity (e.g., Kato, Fukue, & Mineshige 2008. W05 examined the observed spectra for various mass accretion rates and included the effect of disc geometry. They found that the radiation flux is proportional to $\cos\theta$ for the sub-Eddington regime, $\dot{m}_{\rm BH} = 1$–10, where θ is the polar angle (see Fig. 1). The factor $\cos\theta$ represents the change of the effective area via a change of θ, i.e., the projection effect. For a super-Eddington accretion disc with $\dot{m}_{\rm BH} \geqslant 10^2$, although the radiation flux is also proportional to $\cos\theta$ at $\theta < 45^\circ$, it decreases more significantly as θ increases in regions with $\theta \geqslant 45^\circ$.

The bolometric luminosity of an accretion disc is expressed as a function of $\dot{m}_{\rm BH}$ (Watarai, Fukue, & Takeuchi 2000) as follows:

$$L_{\rm bol,disc} = \begin{cases} 2\left(1+\ln\frac{\dot{m}_{\rm BH}}{20}\right) L_{\rm Edd} \ \ (\dot{m}_{\rm BH} \geqslant 20), \\ \left(\frac{\dot{m}_{\rm BH}}{10}\right) L_{\rm Edd} \ \ \ (\dot{m}_{\rm BH} < 20). \end{cases} \tag{1}$$

Based on the results of W05, we can describe the radiation flux from the accretion disc, $F(\theta)$, as follows:

For $\theta < 45^\circ$,

$$F(\theta) = \frac{L_{\rm bol,disc}}{4\pi r^2} \begin{cases} 2\cos\theta \ \ (\dot{m}_{\rm BH} = 1, 10), \\ \frac{20}{7}\cos\theta \ \ (\dot{m}_{\rm BH} = 10^2), \\ \frac{10}{3}\cos\theta \ \ (\dot{m}_{\rm BH} = 10^3). \end{cases} \tag{2}$$

For $\theta \geqslant 45^\circ$,

$$F(\theta) = \frac{L_{\rm bol,disc}}{4\pi r^2} \begin{cases} 2\cos\theta \ \ (\dot{m}_{\rm BH} = 1, 10), \\ \frac{40\sqrt{2}}{7}\cos^4\theta \ \ (\dot{m}_{\rm BH} = 10^2), \\ \frac{160}{3}\cos^9\theta \ \ (\dot{m}_{\rm BH} = 10^3), \end{cases} \tag{3}$$

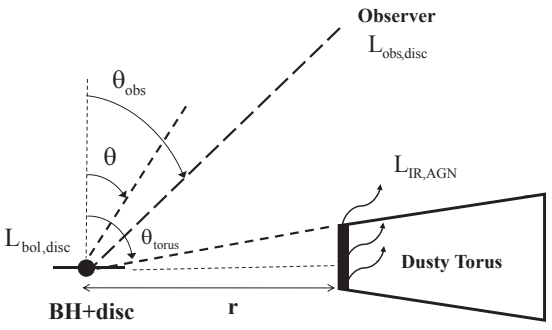

Figure 1. Model for a dusty torus around an SMBH plus an accretion disc. $L_{\rm bol,disc}$ is the bolometric luminosity of the accretion disc and θ is the polar angle. $\theta_{\rm torus}$, r and $L_{\rm IR,AGN}$ are the half opening angle of the torus, the distance from the BH and the infrared luminosity re-emitted by the inner edge of the dusty torus, respectively. $\theta_{\rm obs}$ is the inclination angle.

where r is the distance from the central BH. The coefficients of the cosine functions (see eqs. (2) and (3)) are determined by setting the integral of $F(\theta)$ to be equal to $L_{\rm bol,disc}$ (see eq. (1)) and the continuity of the radiation flux $F(\theta)$ at $\theta = 45^\circ$. We should note that eqs. (2) and (3) well reproduce the results of W05 (see Fig. 3 in W05).

Note that we do not take the corona into account in the present study(but see §4.2). Although X-ray observations have shown the radiation from the disc to be comptonized at the corona above the disc, the size and geometries of the corona are still open questions (e.g., Kubota & Done 2004). The optical thickness of the corona is thought to be around unity or less in the case of sub-Eddington discs (e.g., Kawanaka, Kato, & Mineshige 2008). Hence, the θ-dependence of the radiative flux should not change much. Global radiation hydrodynamic simulations of super-Eddington flows have revealed that the radiative flux is highly collimated, although hot rarefied plasma (corona) appears above the disc (Ohsuga et al. 2005). Recently, similar results have been found by global radiation magnetohydrodynamic simulations (Ohsuga et al. 2009). Thus, we assume that the radiative flux of the sub-Eddington disc is proportional to $\cos\theta$ and employ the collimated radiative flux from the super-Eddington disc in the present study.

3 SIGNATURE OF SUPER-EDDINGTON ACCRETION FLOWS IN AGNS

3.1 Infrared luminosity

In order to examine the AGN IR properties for various mass accretion rates, we model a dusty torus around an SMBH plus an accretion disc system (Fig. 1). Assuming that the radiation of the accretion disc is absorbed by the dust and the AGN IR radiation is re-emitted isotropically at the inner edge of the torus, the AGN IR luminosity ($L_{\rm IR,AGN}$) depends on only the half opening angle of the torus, $\theta_{\rm torus}$, and is independent of the structure of the inner edge of the torus. In other words, energy conservation holds at the inner edge of the torus. Then, $L_{\rm IR,AGN}(\theta_{\rm torus})$ can be given by

$$L_{\rm IR,AGN}(\theta_{\rm torus}) = 4\pi r^2 \int_{\theta_{\rm torus}}^{\pi/2} F(\theta)\sin\theta d\theta. \quad (4)$$

where r is the distance from the central BH. Note that eq. (4) is valid even in a clumpy model (e.g., Nenkova, Ivezić, & Elitzur 2002; Nenkova et al. 2008; Wada & Norman 2002; Hönig et al. 2006; Mor, Netzer, & Elitzur 2009) since there are several optically thick clouds along the line of sight and thus all the radiation of the accretion disc is absorbed by clouds near a BH .

Substituting eqs. (2) and (3) into eq. (4), the ratio of the AGN IR luminosity and the bolometric luminosity is obtained as follows:

For $\theta_{\rm torus} < 45^\circ$,

$$\frac{L_{\rm IR,AGN}}{L_{\rm bol,disc}} = \begin{cases} \cos^2\theta_{\rm torus}, & (\dot{m}_{\rm BH} = 1, 10), \\ \frac{10}{7}\left(\cos^2\theta_{\rm torus} - \frac{3}{10}\right), & (\dot{m}_{\rm BH} = 10^2), \\ \frac{5}{3}\left(\cos^2\theta_{\rm torus} - \frac{2}{5}\right), & (\dot{m}_{\rm BH} = 10^3). \end{cases} \quad (5)$$

For $\theta_{\rm torus} \geqslant 45^\circ$,

$$\frac{L_{\rm IR,AGN}}{L_{\rm bol,disc}} = \begin{cases} \cos^2\theta_{\rm torus}, & (\dot{m}_{\rm BH} = 1, 10), \\ \frac{8\sqrt{2}}{7}\cos^5\theta_{\rm torus}, & (\dot{m}_{\rm BH} = 10^2), \\ \frac{16}{3}\cos^{10}\theta_{\rm torus}, & (\dot{m}_{\rm BH} = 10^3). \end{cases} \quad (6)$$

These relations are understood in terms of the projection effect, self-occultation and the covering factor of the dusty torus. For $\dot{m}_{\rm BH} = 1$–10, the self-occultation effect does not occur because the disc is geometrically thin. Since the radiation flux is reduced by the projection effect, $F(\theta) \propto \cos\theta$ (see eqs. (2) and (3)), and since the covering factor of the torus is given by $4\pi\cos\theta_{\rm torus}$, the IR luminosity decreases with an increase of $\theta_{\rm torus}$. The radiation flux is more sensitive to the polar angle in super-Eddington accretion discs with $\dot{m}_{\rm BH} \geqslant 10^2$ than in sub-Eddington accretion discs via the self- occultation effect (see eqs. (2) and (3)). Hence, the IR luminosity for $\dot{m}_{\rm BH} = 10^2$ and 10^3 drastically decrease as the half opening angle increases when $\theta_{\rm torus} \geqslant 45^\circ$ (see eq. (6)).

In Fig. 2, we plot the ratio of the IR luminosity to the bolometric luminosity, $L_{\rm IR,AGN}/L_{\rm bol,disc}$, against $\theta_{\rm torus}$ for various $\dot{m}_{\rm BH}$. As mentioned above, $L_{\rm IR,AGN}/L_{\rm bol,disc}$ decreases with $\theta_{\rm torus}$ for any $\dot{m}_{\rm BH}$, and this trend is much stronger as $\dot{m}_{\rm BH}$ becomes larger. Super-Eddington AGNs with $\dot{m}_{\rm BH} \geqslant 10^2$ have much smaller ratios of the IR and bolometric luminosities than sub-Eddington AGNs. Although the ratios of $L_{\rm IR,AGN}/L_{\rm bol,disc}$ for $\dot{m}_{\rm BH} = 10^2$ and 10^3 are only a few times smaller than that for $\dot{m}_{\rm BH} = 1$–10 in the case of $\theta_{\rm torus} \approx 45^\circ$, they are one or two orders of magnitude lower than that for $\dot{m}_{\rm BH} \leqslant 10$ in a wide range of half opening angle, $\theta_{\rm torus} > 65^\circ$. We also find that it is hard for sub-Eddington AGNs to achieve a low $L_{\rm IR,AGN}/L_{\rm bol,disc}$, e.g., $L_{\rm IR,AGN}/L_{\rm bol,disc} < 10^{-2}$, unless the obscuring structure is extremely geometrically thin, e.g., $\theta_{\rm torus} > 85^\circ$. In contrast, we find $L_{\rm IR,AGN}/L_{\rm bol,disc} < 10^{-2}$ when $\theta_{\rm torus} > 65^\circ$ for $\dot{m}_{\rm BH} = 10^2$ and when $\theta_{\rm torus} > 55^\circ$ for $\dot{m}_{\rm BH} = 10^3$. Thus, except for an extremely thin torus, a low $L_{\rm IR,AGN}/L_{\rm bol,disc}(< 10^{-2})$ is a signature of the occurrence of super-Eddington accretion flow with $\dot{m}_{\rm BH} \geqslant 10^2$.

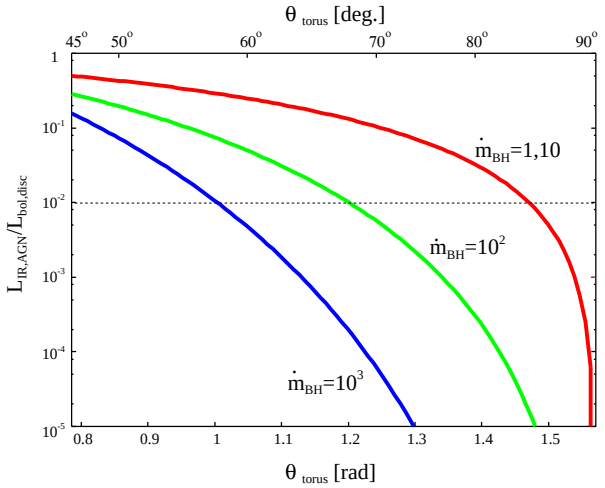

Figure 2. $L_{\rm IR,AGN}/L_{\rm bol,disc}$ against $\theta_{\rm torus}$ for various $\dot{m}_{\rm BH}$. The red line corresponds to $\dot{m}_{\rm BH}=1,10$, the green line shows the case for $\dot{m}_{\rm BH}=10^2$ and the blue line represents the case for $\dot{m}_{\rm BH}=10^3$.

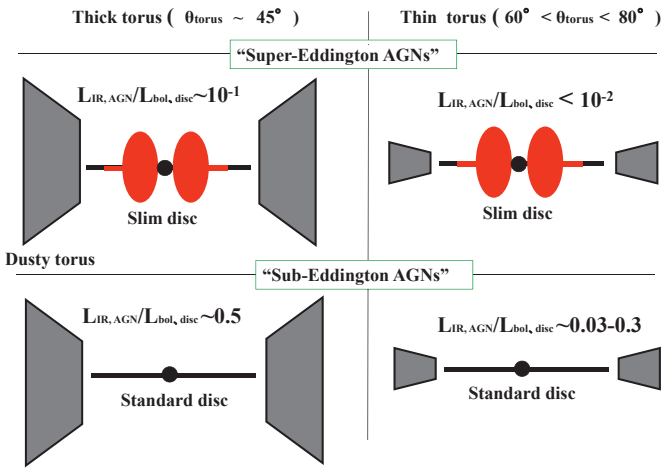

Figure 3. Summary of the dependence of $L_{\rm IR,AGN}/L_{\rm bol,disc}$ on the mass accretion rate into an SMBH and the geometry of the dusty torus. Typical values of $L_{\rm IR,AGN}/L_{\rm bol,disc}$ (see Fig. 2) are shown in each panel. "Super-Eddington AGNs" are expressed as AGNs with $\dot{m}_{\rm BH}\geqslant 10^2$ and "sub-Eddington AGNs" are expressed as AGNs with $\dot{m}_{\rm BH}=1,10$.

These results are summarized as a schematic diagram in Fig. 3. The bottom left panel represents sub-Eddington accretion with a thick torus. In this case, $L_{\rm IR,AGN}/L_{\rm bol,disc}$ is maximal. For super-Eddington accretion ($\dot{m}_{\rm BH}\geqslant 10^2$) with a thick torus (top left panel), $L_{\rm IR,AGN}/L_{\rm bol,disc}$ is slightly smaller than the bottom left panel due to the self-occultation effect. For sub-Eddington accretion with a thin torus (bottom right panel), $L_{\rm IR,AGN}/L_{\rm bol,disc}$ becomes smaller than the case of the bottom left panel, because the radiation of the accretion disc is reprocessed at the small inner surface of the torus. Super-Eddington accretion ($\dot{m}_{\rm BH}\geqslant 10^2$) with a thin torus (top right panel) has the smallest $L_{\rm IR,AGN}/L_{\rm bol,disc}$ in the four panels of Fig. 3 due to the self-occultation effect of the disc along with the small covering factor of the torus.

We here mention the effect of the inclination angle, $\theta_{\rm obs}$ (Fig. 1). The observed ratio $L_{\rm IR,AGN}/L_{\rm obs,disc}(\theta_{\rm obs})$ depends on $\theta_{\rm obs}$, but $L_{\rm IR,AGN}$ is independent of $\theta_{\rm obs}$, where $L_{\rm obs,disc}(\theta_{\rm obs})$ is the observed disc luminosity at the viewing angle of $\theta_{\rm obs}$. However, the difference between $\theta_{\rm obs}=0^\circ$ (face on) and $\theta_{\rm obs}$=30° is a factor of $\sqrt{3}/2$. In contrast, in the case of 45 deg $<\theta_{\rm obs}<\theta_{\rm torus}$, the dependence of $\theta_{\rm obs}$ on $F(\theta_{\rm obs})$ is sensitive to $\dot{m}_{\rm BH}$. For example, the difference between $\theta_{\rm obs}$=0° (face on) and $\theta_{\rm obs}$=60 ° is a factor of 1/2, $\sqrt{2}/8$ and 1/32 for $\dot{m}_{\rm BH}$ = 1–10, 10^2 and 10^3, respectively. Thus, when $\theta_{\rm obs}>45$ deg, the IR luminosity of super-Eddington AGNs could be similar to that of sub-Eddington AGNs.

In summary, the IR luminosity of super-Eddington AGNs is very faint for $\theta_{\rm obs}<45^\circ$, while it is not so faint for $45^\circ<\theta_{\rm obs}<\theta_{\rm torus}$. Therefore, in order to examine the candidate super-Eddington AGNs effectively by IR observations, it is worth constructing samples of pure type 1 AGNs (i.e., $\theta_{\rm obs}<45^\circ$) rather than type 1.5 and 1.8 AGNs.

In this paper, we assume that the dusty torus is aligned with the accretion disc, such as in Fig. 1. However, this is not a trivial assumption because it is unclear whether the dusty torus is a reservoir of the gas which accretes onto the accretion disc. If the accretion disc is misaligned with the dusty torus, the self-occultation effect becomes less important as the angle between the rotation axis of the accretion disc and that of the torus increases (see eqs. (2) and (3)), since a large number of photons from the accretion disc are absorbed and re-emitted at the dusty torus. Thus, the ratio $L_{\rm IR,AGN}/L_{\rm bol,disc}$ for super-Eddington AGNs would be comparable to that for sub-Eddington AGNs.

Lastly, we note the relation between the AGN type and $\theta_{\rm torus}$. It may be questioned whether our method is worthwhile if the AGN types are mainly determined by $\theta_{\rm torus}$ and $\theta_{\rm torus}=45^\circ$ is a standard torus model for all types of AGN. However, recent observations on circum-nuclear regions of AGNs have revealed that type 2 Seyferts are more frequently associated with starbursts than type 1 Seyferts (e.g., Heckman et al. 1989; Maiolino et al. 1997; Perez-Olea & Colina 1996; Hunt et al. 1997; Malkan, Gorjian, & Tam 1998; Schmitt, Storchi-Bergmann, & Cid Fernandes 1999; Storchi-Bergmann et al. 2000; González Delgado, Heckman, & Leitherer 2001). In addition, the fraction of type 2 AGNs decreases with AGN luminosity (e.g., Ueda et al. 2003; Maiolino et al. 2007; Hasinger 2008). These findings imply that the type1/type2 ratio is not simply determined by the opening angle ($\theta_{\rm torus}$). Moreover, the formation mechanism of the obscuring torus is still a hotly debated issue theoretically (e.g., Krolik & Begelman 1988; Pier & Krolik 1992; Ohsuga & Umemura 1999, 2001; Wada & Norman 2002; Watabe & Umemura 2005; Schartmann et al. 2009). Thus, even if the effect we proposed becomes significant only for relatively large $\theta_{\rm torus}$ ($>65^\circ$), our method is useful for exploring the candidates of super-Eddington AGNs.

3.2 Near-infrared luminosity

Near-IR (NIR) emission is produced by the hot dust (> 1000 K) which is directly heated by the central AGNs,

though the total IR emission may be contaminated by the nuclear starburst. Thus, based on the results of Fig. 2, we investigate the dependence of the ratio $L_{\rm NIR,AGN}/L_{\rm bol,disc}$ on the mass accretion rate, $\dot{m}_{\rm BH}$. The NIR luminosity, $L_{\rm NIR,AGN}$, strongly depends on the shape of the inner edge of the torus, because the hot dust temperature, $T_{\rm d}(\theta)$, is sensitive to the structure of the torus. We here consider the following three typical models for the structure of the inner edge of the torus (see Fig. 4).

First, we examine the case where the inner radius of the torus $r_{\rm in}$ is determined by the sublimation radius $r_{\rm sub}(\theta)$ (Fig. 4(i)). Here $r_{\rm sub}(\theta)$ is defined as the radius where the hot dust temperature is $T_{\rm d}(\theta) = T_{\rm sub} = 1500\,{\rm K}$ where $T_{\rm sub}$ is the silicate grain sublimation temperature (e.g., Barvainis 1987; Laor & Draine 1993; Suganuma et al. 2006). If this is the case, the sublimation radius could be elongated to extend to the central BH in the equatorial plane (see Kawaguchi & Mori 2010), since the dust in the equatorial plane can survive because $T_{\rm d}(\theta > \theta_{\rm torus}) < T_{\rm sub}$. Since such dust particles at $r_{\rm sub}(\theta > \theta_{\rm torus})$ can be heated to ∼1500 K due to illumination and emit NIR (see Fig. 4 (i)), the NIR luminosity is equal to the IR luminosity, i.e., $L_{\rm NIR,AGN} = L_{\rm IR,AGN}$ for all $\dot{m}_{\rm BH}$. Thus, we can just replace $L_{\rm IR,AGN}/L_{\rm bol,disc}$ assigned at the vertical axis in Fig. 2. with $L_{\rm NIR,AGN}/L_{\rm bol,disc}$.

Second, we consider the case where the NIR emission comes from only a small part of the inner edge (Fig. 4(ii)). In this case, we define the NIR luminosity ($L_{\rm NIR,AGN}$) as the luminosity emitted by the hot dust ($T_{\rm d} = 1000$–$1500\,{\rm K}$). The NIR luminosity is obtained as $L_{\rm NIR,AGN} = \left(\frac{\cos\theta_{\rm torus} - \cos\theta_{\rm hot}}{\cos\theta_{\rm torus}}\right) L_{\rm IR,AGN}$ where $\theta_{\rm hot}$ is defined as $T_{\rm d}(\theta_{\rm hot}) = 1000\,{\rm K}$, as seen in Fig. 4(ii). The contribution of NIR emission decreases as the mass accretion rate is high, because for a large $\dot{m}_{\rm BH}$ the hot region at the inner edge of the torus (the red shaded region in Fig. 4(ii)) becomes smaller due to self-occultation of the super-Eddington accretion flow. As a result, we find that for a given $\theta_{\rm torus}$, the ratio $L_{\rm NIR,AGN}/L_{\rm IR,AGN}$ for super-Eddington AGNs with $\dot{m}_{\rm BH} \geqslant 10^2$ is much smaller than that for sub-Eddington AGNs with $\dot{m}_{\rm BH} = 1$–10, as shown in Table 1.

Third, we consider the case where the dust temperature of the whole inner edge of the torus becomes lower than $T_{\rm sub}$ (Fig. 4(iii)). If this is the case, it is expected that there will be no NIR emission from the dusty torus for both sub- and super-Eddington AGNs. However, this prediction is in conflict with NIR observations of sub-Eddington AGNs (e.g., Elvis et al. 1994; Glikman, Helfand, & White 2006). Thus, only for NIR-faint AGNs, the dust temperature at $r_{\rm in}$ might be below the dust sublimation temperature, because the inner radius is larger than the expected sublimation radius. To investigate this possibility, for NIR-faint AGNs, it is important to evaluate the time lag between the UV and NIR light by photometric monitoring observations (e.g., Glass 2004; Minezaki et al. 2004; Suganuma et al. 2006).

Taking into account the above results, we can conclude that a relatively low $L_{\rm NIR,AGN}/L_{\rm bol,disc}$, as well as $L_{\rm IR,AGN}/L_{\rm bol,disc}$, is a sign of super-Eddington AGNs with $\dot{m}_{\rm BH} \geqslant 10^2$, unless the half opening angle of the torus is small ($\theta_{\rm torus} < 65^\circ$). We can also confirm that the predicted $L_{\rm NIR,AGN}/L_{\rm bol,disc}$ with $\dot{m}_{\rm BH} = 1$–10 (Fig. 2, see also Table 1) almost coincides with the observed results of sub-Eddington quasars (e.g., Elvis et al. 1994; Glikman, Helfand, & White 2006), assuming $L_{\rm bol,disc} = 9L_{5100}$ where L_{5100} is the AGN luminosity at 5100Å (Kaspi et al. 2000).

Table 1. Dependence of $L_{\rm NIR,AGN}/L_{\rm bol,disk}$ on $\theta_{\rm torus}$ and $\dot{m}_{\rm BH}$

—	$\theta_{\rm torus} = 45^\circ$	60°	80°
$\dot{m}_{\rm BH} = 1, 10$	0.38	0.19	0.02
10^2	0.08	0.01	8.4×10^{-5}
10^3	0.028	8.3×10^{-4}	2.2×10^{-8}

Finally, we discuss the evaporation of nearby dusty clouds irradiated by AGNs. In the steady state for a dusty torus, cloud evaporation at the inner radius of the torus should balance the mass supply of the clouds from the outer region (see Krolik & Begelman 1988). If the evaporation timescale, $t_{\rm evap}$, is longer than the orbital period of a cloud around SMBHs, $t_{\rm orb}$, the inner radius is determined by the sublimation radius, $r_{\rm sub}$. On the other hand, when $t_{\rm evap} \leqslant t_{\rm orb}$, the evaporation could be determined by the location of the inner edge of the torus. Thus, the inner radius of the dusty torus becomes larger than the sublimation radius. If this is the case, the NIR luminosity could be overestimated because the dust temperature is lower. To check this, we estimate the two timescales ($t_{\rm evap}$ and $t_{\rm orb}$) for the present model. Assuming $r_{\rm sub} = 1.3L_{46}^{1/2}T_{\rm sub}^{-2.6}$, the orbital period of a cloud at $r_{\rm sub}$ is

$$\begin{aligned} t_{\rm orb} &= 2\pi r_{\rm sub}/v_\phi \\ &= 4.5\times10^4 L_{46}^{1/4}(L_{\rm bol,disc}/L_{\rm Edd})^{1/2}\,{\rm yr}, \end{aligned} \quad (7)$$

where v_ϕ is the rotational velocity and $L_{46} = L_{\rm bol,disc}/10^{46}\,{\rm erg\,s^{-1}}$. Following Pier & Voit (1995), for a cloud of mass $M_{\rm c} = 10M_\odot$ and $T_{\rm dust} = 1500\,{\rm K}$, the evaporation timescale is given by

$$t_{\rm evap} = 2.8\times10^5 (F(\theta_{\rm torus})/10^8\,{\rm ergs\,cm^{-2}\,s^{-1}})^{-0.19}. \quad (8)$$

Note that $F(\theta_{\rm torus} = 45^\circ)$ at $r_{\rm sub}$ is $\approx 10^8\,{\rm ergs\,cm^{-2}\,s^{-1}}$ (eqs.(2) and (3)). Comparing these two timescales, we find $t_{\rm evap} \gg t_{\rm orb}$ for sub-Eddington AGNs with $\dot{m}_{\rm BH} = 1, 10$(see Pier & Voit 1995 in details). On the other hand, for super-Eddington AGNs with $\dot{m}_{\rm BH} = 10^3$ and $L_{\rm bol,disc} > 10^{46}\,{\rm ergs\,s^{-1}}$, the evaporation timescale is comparable to the orbital period of a cloud, i.e., $t_{\rm evap} \approx t_{\rm orb}$ (see eqs. (7) and (8)). If this is the case, evaporation of a dusty cloud would be fast enough to reduce the overall NIR emission. Therefore, AGNs with high $L_{\rm bol}$ and $\dot{m}_{\rm BH}$, such as bright narrow-line quasars, might have a much smaller ratio $L_{\rm NIR}/L_{\rm bol,disc}$, compared to the results of Fig. 2.

4 DISCUSSIONS

4.1 IR emission from NLR clouds

So far, we have not taken into account the IR emission from narrow-line region (NLR) clouds. However, it is known that dust grains are present in the NLR of Seyferts (e.g., Dahari & De Robertis 1988; Netzer & Laor 1993). Thus, the dusty clouds in the NLR might be a source of IR emission and hence we must consider the contribution of IR emission from NLR clouds.

NLR clouds are assumed to be distributed in a geometrically thin spherical shell with radius $r_{\rm NLR}$ in the range $0 \leqslant \theta \leqslant \theta_{\rm torus}$. Assuming the covering factor of the NLR clouds, $f_{\rm NLR}$, and the optical depth of the NLR clouds, $\tau_{\rm NLR}$, the IR luminosity from NLR clouds can be given by

$$L_{\rm IR,NLR} = 4\pi r_{\rm NLR}^2 f_{\rm NLR}(1-e^{-\tau_{\rm NLR}}) \int_0^{\theta_{\rm torus}} F(\theta)\sin\theta d\theta. \\ = f_{\rm NLR}(1-e^{-\tau_{\rm NLR}}) \left(1-\frac{L_{\rm IR,AGN}}{L_{\rm bol,disc}}\right), \quad (9)$$

where $L_{\rm IR,AGN}/L_{\rm bol,disc}$ is a function of $\theta_{\rm torus}$ (see eqs. (5) and (6)). In Fig. 4, we plot the ratio of the IR luminosity to the bolometric luminosity against $\theta_{\rm torus}$ for the NLR clouds, assuming $\tau_{\rm NLR} = 1$ and $f_{\rm NLR} = 0.1$. Note that the dust extinction of NLR emission is small (i.e., $\tau_{\rm NLR} \leqslant 1$) for type 1 AGNs (Rodríguez-Ardila, Pastoriza, & Donzelli 2000) and the typical covering factor is about 10% (e.g., Netzer & Laor 1993; Baskin & Laor 2005).

Figure 4 shows that the IR emission from the NLR clouds dominates above $\theta_{\rm torus} = 75^\circ$ for $\dot{m}_{\rm BH} = 1, 10$, while for $\dot{m}_{\rm BH} = 10^2$ and $\dot{m}_{\rm BH} = 10^3$ the IR emission from NLR clouds is important above $\theta_{\rm torus} = 60^\circ$ and $\theta_{\rm torus} = 50^\circ$, respectively. This suggests that for super-Eddington AGNs with $\dot{m}_{\rm BH} \geqslant 10^2$, the IR emission from NLR clouds can dominate the IR emission from the dusty torus. This is because the radiative flux of super-Eddington AGNs is highly collimated compared to sub-Eddington AGNs (see eqs. (2) and (3)). However, we should mention that the NLR size, $r_{\rm NLR}$, is about 10^2 times as large as the sublimation radius (e.g., Bennert et al. 2002; Netzer et al. 2004; Baskin & Laor 2005) and the dust temperature of NLR clouds is lower than the hottest dust temperature (i.e., 1500 K). Thus, the IR emission from NLR clouds would contribute mainly MIR (10–30 μm) emission (see Schweitzer et al. 2008; Mor, Netzer, & Elitzur 2009). In order to avoid contamination of the IR emission from NLR clouds, the ratio $L_{\rm NIR,AGN}/L_{\rm bol,disc}$ can be used to probe an inflated disk due to super-Eddington accretion, as mentioned in §3.2.

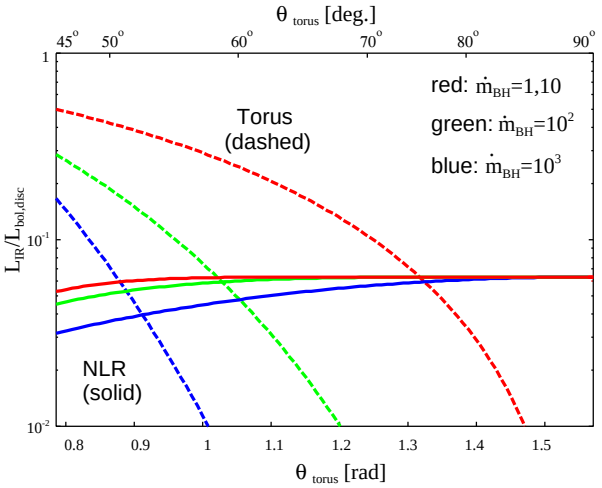

Figure 4. $L_{\rm IR,AGN}/L_{\rm bol,disc}$ against $\theta_{\rm torus}$ for various $\dot{m}_{\rm BH}$. The solid lines show the ratio of the IR luminosity and bolometric luminosity for the NLR clouds, assuming $\tau_{\rm NLR} = 1$ and $f_{\rm NLR} = 0.1$. The dashed lines show $L_{\rm IR}/L_{\rm bol,disc}$ for the dusty torus (see Fig. 2).

4.2 Contribution of X-ray emission from the corona

We here discuss the contribution of X-ray emission from the corona on the IR emission. For the model of X-ray emission from the corona, we adopt a simple lamp-post geometry model, where the X-ray source is located above the SMBH at some height $h_{\rm x}$ (e.g., George & Fabian 1991; Nayakshin & Kallman 2001). First, we examine the condition where the X-ray emission can reach the torus inner edge for super-Eddington accretion when $\theta_{\rm torus} \geqslant 45^\circ$. If the light ray, which passes though the maximum thickness of the slim disc $h_{\rm slim}$ from the X-ray source located at $h_{\rm x}$, hits the torus inner edge, $r_{\rm sub}$, a large amount of X-ray emission is absorbed by the dust torus. Assuming $r_{\rm sub} \gg r_{\rm slim}$, this condition can be simply expressed by the following:

$$\frac{h_{\rm x}}{h_{\rm slim}} > 1 - \tan(90^\circ - \theta_{\rm torus}), \quad (10)$$

where $r_{\rm slim}$ is the radius of the slim disc and $h_{\rm slim} = r_{\rm slim}$ because the half opening angle of the slim disc is 45° (see §2). For example, the X-ray emission could produce the IR emission, if $h_{\rm x} > 0.4h_{\rm slim}$ and $h_{\rm x} > 0.8h_{\rm slim}$ for $\theta_{\rm torus} = 60^\circ$ and 80°, respectively. According to the theory of slim discs, $r_{\rm slim}$ is about $10r_{\rm g}$ for $\dot{m}_{\rm BH} = 10^2$. Note that for $\dot{m}_{\rm BH} = 10^3$, $r_{\rm slim}$ is much larger than $10r_{\rm g}$ (e.g., Watarai, Fukue, & Takeuchi 2000). This may imply that the contribution of X-rays from the corona is not negligible if $h_{\rm x}$ is larger than 4–8$r_{\rm g}$. The lower limit of $h_{\rm x}$ is comparable to $h_{\rm x} = 6r_{\rm g}$, which is frequently used to discuss the iron-line reverberation in AGNs (e.g., Reynolds & Begelman 1997).

We next investigate the contribution of X-rays from the corona on the IR emission when $h_{\rm x} > (4\text{–}8)r_{\rm g}$. The ratio of the radiation flux from the accretion disc, $F_{\rm disc}$, and the corona, $F_{\rm cor}$, at $\theta_{\rm torus}$ is expressed as

$$\frac{F_{\rm disc}}{F_{\rm cor}} = \left(\frac{L_{\rm bol,disc}}{L_{\rm x}}\right)\left(\frac{r_{\rm x}}{r_{\rm sub}}\right)^2 \begin{cases} 2\cos\theta_{\rm torus} & (\dot{m}_{\rm BH} = 1, 10), \\ \frac{40\sqrt{2}}{7}\cos^4\theta_{\rm torus} & (\dot{m}_{\rm BH} = 10^2), \\ \frac{160}{3}\cos^9\theta_{\rm torus} & (\dot{m}_{\rm BH} = 10^3). \end{cases} \quad (11)$$

Here $r_{\rm x} (\geqslant r_{\rm sub})$ is the distance from the X-ray source to the inner radius of the dusty torus. Assuming that the X-ray emission is isotropic, it is found that as $\theta_{\rm torus}$ and $\dot{m}_{\rm BH}$ increase, the X-ray emission from the corona begins to contribute to the IR emission from the dusty torus. However, we should keep in mind that the dust opacity for X-ray radiation is lower than that for optical-UV radiation (e.g., Draine & Lee 1984; Laor & Draine 1993). Thus, the evaluated contribution of X-rays from the corona could be overestimated.

4.3 Physical models of the dusty torus

In §3.2, we considered three typical models for the configuration of the inner edge of the dusty torus (see Fig. 5). We here discuss how these three types can be understood physically. The following two physical quanti-

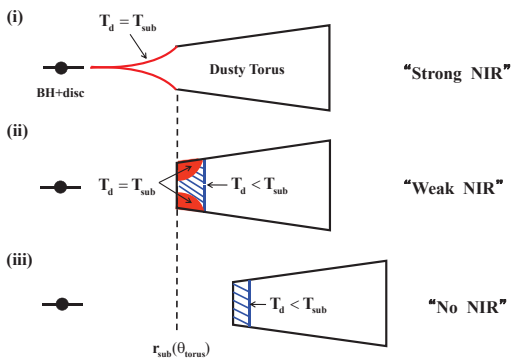

Figure 5. Three typical models for the shape of the inner edge of the torus. $T_{\rm d}$ and $T_{\rm sub}$ are the dust temperature and sublimation temperature, respectively. Note that $r_{\rm sub}(\theta_{\rm torus})$ is the sublimation radius at $\theta = \theta_{\rm torus}$. The red thick lines and shaded portions denote the region of NIR emission (i.e., $T_{\rm d} = T_{\rm sub}$). The blue shaded portions show the region of no NIR emission (i.e., $T_{\rm d} < T_{\rm sub}$).

ties may be closely related to the shape of the inner part of the dusty torus. One is the sublimation radius, $r_{\rm sub}(\theta)$, which determines the region where hot dust can survive. In order to maintain a geometrically thick structure, energy input from stars and/or supernovae in the dusty torus is necessary (e.g., Wada & Norman 2002; Thompson, Quataert, & Murray 2005; Kawakatu & Wada 2008). This energy input may occur outside of the critical radius, r_*, above which the torus is gravitationally unstable, if we adopt Toomre's stability criterion. Thus, the magnitude relation between $r_{\rm sub}(\theta_{\rm torus})$ and r_* may determine the structure of the inner part of the dusty torus, as in the following three cases. (i) If $r_* \ll r_{\rm sub}(\theta_{\rm torus})$, the inner radius of the torus, $r_{\rm in}$, may be determined by $r_{\rm sub}(\theta)$. This corresponds to the case of Fig. 5(i). (ii) When $r_* \approx r_{\rm sub}(\theta_{\rm torus})$, the structure of the dusty torus is like Fig. 5(ii). As mentioned above, the dust can survive at even $r < r_{\rm sub}(\theta_{\rm torus})$, though the structure within r_* is geometrically thin because there is no energy source in this region. Thus, the NIR emission from $r < r_*$ is negligible since the covering factor becomes small. That is, $r_{\rm in}$ is determined by the radius for which the dusty torus is gravitationally unstable. (iii) If $r_* \gg r_{\rm sub}(\theta_{\rm torus})$, the dust temperature of the whole inner edge of the dusty torus becomes lower than $T_{\rm sub}$ because $r_{\rm in} = r_*$ is much larger than $r_{\rm sub}(\theta)$. If this is the case, the structure of the dusty torus is similar to Fig. 5(iii). By exploring the relation between the region of nuclear starbursts and that of the hot dust, we may find evidence revealing the formation of the dusty torus.

4.4 Evolutionary tracks in $L_{\rm IR,AGN}/L_{\rm bol,disc} - \theta_{\rm torus}$ plane

We now discuss the evolutionary tracks of SMBH growth in the $L_{\rm IR,AGN}/L_{\rm bol,disc}$–$\theta_{\rm torus}$ diagram. As mentioned in §3.1, although the formation mechanism of the obscuring torus is still a hotly debated issue (e.g., Krolik & Begelman 1988; Pier & Krolik 1992; Ohsuga & Umemura 1999, 2001; Wada & Norman 2002; Watabe & Umemura 2005; Wada, Papadopoulos, & Spaans 2009; Schartmann et al. 2009), Wada & Norman (2002) proposed a dusty torus supported by turbulent pressure, in which the turbulence is produced by SN explosions (see also Kawakatu & Wada 2008; Wada, Papadopoulos, & Spaans 2009). In their model, the geometrical thickness of the torus, which is determined by the balance between the gravity of the central BH and the force due to turbulent pressure, is smaller for more massive BHs. This tendency is consistent with observations in which the covering factor of the dusty torus decreases with increasing BH mass (e.g., Maiolino et al. 2007; Noguchi et al. 2010). This model also implies that $\theta_{\rm torus}$ increases with time as the BH grows. That is, the evolution proceeds from left to right in the $L_{\rm IR,AGN}/L_{\rm bol,disc}$–$\theta_{\rm torus}$ diagram (see Fig. 5). Here we consider two simple scenarios: (i) the super-Eddington growth dominated scenario where most of the mass of the SMBHs is supplied not through sub-Eddington accretion discs but through super-Eddington accretion discs. (ii) the sub-Eddington growth dominated scenario where the sub-Eddington accretion disc mainly feeds the SMBH. Figure 6 shows the evolutionary tracks for these two scenarios, assuming an initial opening angle of the torus of $\theta_{\rm torus,init} = 45^\circ$ and initially $\dot{m}_{\rm BH} = 10^3$. We find from this figure that the AGNs stay in a super-Eddington phase ($\dot{m}_{\rm BH} > 10^2$) for a long time (a wide range of $\theta_{\rm torus}$) in case (i), whereas in case (ii) the AGNs shift to a sub-Eddington phase when the torus is relatively thick. The two distinct scenarios can be clearly understood from Fig. 3 as follows: for case (i) the evolution proceeds from top left → top right → bottom right, whereas for case (ii) it goes from top left → bottom left → bottom right. That is, the AGNs never undergo a phase of extremely low $L_{\rm IR,AGN}/L_{\rm bol,disc}$ for case (ii). In contrast, in case (i), many AGNs can be identified as IR faint objects. The NIR luminosity of such AGNs is also very small. The dispersion of $L_{\rm IR,AGN}/L_{\rm bol,disc}$ as well as $L_{\rm NIR,AGN}/L_{\rm bol,disc}$ for case (i) is significantly larger than that for case (ii). If the majority of high-z quasars ($z > 7$) are NIR-faint, super-Eddington growth may be inevitable for SMBH growth in the early Universe. In order to compare the predictions with observations in detail, we must elucidate the evolution of $L_{\rm NIR,AGN}/L_{\rm bol,disc}$ based on the coevolution model of SMBH growth and a circumnuclear disc such as Kawakatu & Wada (2008). This is a subject for future work.

4.5 Comparison with observations

In this paper, we predicted that super-Eddington AGNs with $\dot{m}_{\rm BH} \geqslant 10^2$ have relatively low $L_{\rm NIR,AGN}/L_{\rm bol,disc}$. So far, more than 30 quasars have been discovered at $z \approx 6$ (e.g., Fan et al. 2001, 2006; Goto 2006; Willott et al. 2007, 2010). Jiang et al. (2010) found that two are unusually NIR-faint quasars, i.e., their ratio of $L_{\rm NIR}/L_{5100}$ is one order of magnitude smaller than the average for ordinary quasars, although their properties are similar to those of low-z quasars in the rest-frame ultraviolet/optical and X-ray bands (e.g., Fan et al. 2004; Jiang et al. 2006; Shemmer et al. 2006). More interestingly, the two quasars have the smallest BH mass ($M_{\rm BH} \approx 10^8 M_\odot$) and the highest Eddington ratios ($L_{\rm bol,AGN}/L_{\rm Edd} \sim 2$) of $z \sim 6$ quasar samples. These features can be nicely explained by our interpretation, i.e., the faint NIR emission for high

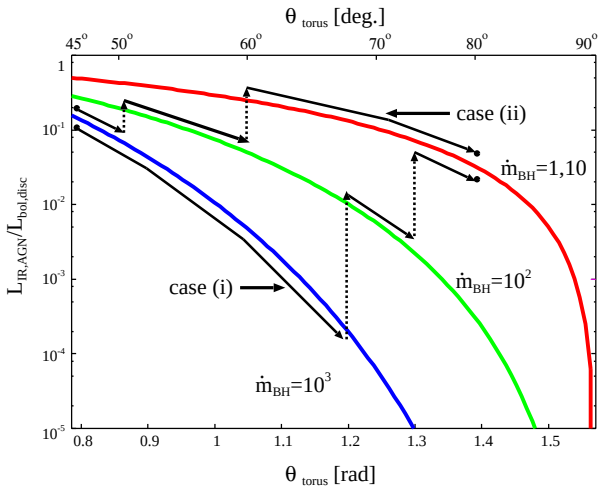

Figure 6. Schematic diagram of two evolutionary scenarios, super-Eddington growth dominated scenario (case (i)) and sub-Eddington growth dominated scenario (case(ii)). The evolution proceeds from left to right, i.e., as the mass of the BH increases, $\theta_{\rm torus}$ increases (see text). We assume that the initial opening angle of the torus is $\theta = 45^\circ$ and $\dot{m}_{\rm BH} = 10^3$.

Eddington AGNs. We should note that since NIR-faint quasars can be explained by sub-Eddington AGNs with extremely thin tori (i.e., $\theta_{\rm torus} > 85^\circ$), we need to measure the thickness of a dusty torus to confirm whether NIR-faint quasars are really super-Eddington AGNs ($\dot{m}_{\rm BH} \geqslant 10^2$). Based on the kinematics of cold molecular gas in a torus, it would be possible to evaluate the thickness of a torus by ALMA, because the ratio of velocity dispersion and rotational velocity indicates the scale height of the torus (see Wada & Norman 2002; Wada & Tomisaka 2005). On the other hand, Jiang et al. (2010) interpreted these two objects as dust-free quasars. However, this seems to contradict the observations, which suggests that NIR-faint quasars possess super-metallicity as do other $z \sim 6$ quasars and high-z AGNs (e.g., Pentericci et al. 2002; Freudling, Corbin, & Korista 2003; Juarez et al. 2009; Hamann & Ferland 1993; Nagao, Maiolino, & Marconi 2006a,b; Matsuoka et al. 2009). Also, Hao et al. (2010) recently reported quasars with unusually faint NIR emission at $z = 1.5$–3, when the universe was 2–4 Gyr old. Thus, it seems likely that NIR-faint quasars are exclusively dust-free AGNs. As an alternative scenario, a large fraction of gas in a dusty torus would be ejected from host galaxies as a result of strong radiation pressure from the brightest AGNs, such as quasars (Ohsuga & Umemura 1999, 2001; Watabe & Umemura 2005). In this case, NIR-faint quasars may be explained as being quasars without dusty tori around the SMBH. This possibility could be confirmed by investigating the presence of dusty tori in NIR-faint quasars using ALMA.

In the local universe, NLS1s are thought to be AGNs of a high $L_{\rm bol,disc}/L_{\rm Edd}$ system. One NLS1 (Ark 564) shows no NIR emission (Rodríguez-Ardila & Mazzalay 2006), which is consistent with our predictions. However, most NLS1s tend to have NIR emission similar to or stronger than that of ordinary Seyfert galaxies (e.g. Ryan et al. 2007). One of the reasons for the discrepancy between our predictions and the observations is that NLS1s with $\dot{m}_{\rm BH} \geqslant 10^2$ may be absent (or their fraction is very small). However, some NLS1s have a high mass accretion rate with $\dot{m}_{\rm BH} \geqslant 10^2$ (e.g., Collin & Kawaguchi 2004; Haba et al. 2008). Another possibility is that these discrepancies may suggest misalignment between the accretion discs and the dusty torus, as mentioned in §3.1. Lastly, we note the possibility of contamination of hosts and circumnuclear starbursts in the NIR band, if the host luminosity is comparable to or exceeds the AGN luminosity, as in Seyfert galaxies. Although it may be hard to find many NLS1s with low $L_{\rm NIR,AGN}/L_{\rm bol,disc}$ in current observations, in future studies it is worth examining this issue by NIR (rest frame) observations with high spatial resolution.

5 SUMMARY

In this work, we propose a new method to search for candidate galaxies in which super-Eddington growth occurs. In particular, taking account of the dependence of the polar angle on the radiation flux of accretion flows, we investigate the properties of reprocessed IR emission (as well as NIR emission) from the inner edge of the dusty torus. As a result, we find that a relatively low ratio of AGN IR (as well as NIR) luminosity and disc luminosity is a genuine property that can be used for exploring for candidates of super-Eddington AGNs with $\dot{m}_{\rm BH} \geqslant 10^2$. This method is especially powerful for searching for high-z super-Eddington AGNs because the direct measurement of $\dot{m}_{\rm BH}$ is difficult for high-z AGNs compared with nearby AGNs.

The following are the main results of the present paper:

(i) We find that the ratio of the AGN IR luminosity, $L_{\rm IR,AGN}$, and the disc bolometric luminosity, $L_{\rm bol,disc}$, decreases as the half opening angle of the dusty torus, $\theta_{\rm torus}$, increases and the mass accretion rate normalized by the Eddington rate, $\dot{m}_{\rm BH}$, increases. The dependence of the ratio on $\dot{m}_{\rm BH}$ is caused by the self-occultation effect, which attenuates the illumination of the torus via the self-absorption of the emission from the inner disc surface at the outer region of super-Eddington accretion discs. The ratio in super-Eddington AGNs with $\dot{m}_{\rm BH} \geqslant 10^2$ is more than one order of magnitude lower than that in sub-Eddington AGNs with $\dot{m}_{\rm BH} = 1$–10 for $\theta_{\rm torus} > 65^\circ$ ($\dot{m}_{\rm BH} = 10^2$) and for $\theta_{\rm torus} > 55^\circ$ ($\dot{m}_{\rm BH} = 10^3$). A small value of $L_{\rm IR,AGN}/L_{\rm bol,disc}$ could be a signature of super-Eddington accretion with $\dot{m}_{\rm BH} \geqslant 10^2$, since it cannot be realized in sub-Eddington AGNs, unless the torus has quite a wide opening angle, $\theta_{\rm torus} > 85^\circ$.

(ii) We also examined the properties of the AGN near-IR luminosity ($L_{\rm NIR,AGN}$) radiated from hot dust at > 1000 K, because it may be hard to detect pure AGN IR emission from the inner edge of a torus because of contamination of the nuclear starburst. In this case, $L_{\rm NIR,AGN}/L_{\rm bol,disc}$ of super-Eddington AGNs with $\dot{m}_{\rm BH} \geqslant 10^2$ is at least one order of magnitude smaller than that for sub-Eddington AGNs over a wide range of half opening angle ($\theta_{\rm torus} \geqslant 65^\circ$). This is true regardless of which of the three typical models of the dusty torus is used.

ACKNOWLEDGMENTS

We appreciate the useful comments of the anonymous referees that reviewed this paper. We are grateful to M. Umemura and T. Nagao for useful comments and discussions. This work is supported in part by the Ministry of Education, Culture, Sports, Science, and Technology (MEXT) Research Activity start-up 2284007 (NK) and Young Scientist (B) 20740115 (KO).

REFERENCES

Abramowicz M. A., Czerny B., Lasota J. P., Szuszkiewicz E., 1988, ApJ, 332, 646
Antonucci R., 1993, ARA&A, 31, 473
Barvainis R., 1987, ApJ, 320, 537
Baskin A., Laor A., 2005, MNRAS, 358, 1043
Begelman M. C., 1978, MNRAS, 184, 53
Bennert N., Falcke H., Schulz H., Wilson A. S., Wills B. J., 2002, ApJ, 574, L105
Boller Th., Brandt W. N., Fink H. H., 1996, A&A, 305, 53
Boller Th., Fabian A. C., Sunyaev R., et al., 2002, MNRAS, 329, L1
Boller Th., Tanaka Y., Fabian A. C., et al., 2003, MNRAS, 343, L89
Brandt N., Boller T., 1998, Astron. Nach., 319, 163
Collin S., Kawaguchi T., 2004, A&A, 426, 797
Collin S., Kawaguchi T., Peterson B. M., Vestergaard M., 2006, A&A, 456, 75
Dahari O., De Robertis M. M., 1988, ApJ, 331, 727
Draine B. T., Lee H. M., 1984, ApJ, 285, 89
Elitzur M., 2008, New Astronomy Review, 52, 274
Elvis M., et al., 1994, ApJS, 95, 1
Fabian A. C., 1999, MNRAS, 308, L9
Fan X., et al., 2001, AJ, 122, 2833
—, 2004, AJ, 128, 515
—, 2006, AJ, 131, 1203
Ferrarese L., Merritt D., 2000, ApJL, 539, L9
Freudling W., Corbin M. R., Korista K. T., 2003, ApJ, 587, L67
Fukue J., 2000, PASJ, 52, 829
Gallo L. C., Boller Th., Tanaka Y., et al. 2004, MNRAS, 347, 269
Gillessen S., Eisenhauer F., Trippe S., Alexander T., Genzel R., Martins F., Ott T., 2009, ApJ, 692,1075
George I. M., Fabian A. C., 1991, MNRAS, 249, 352
Glass I. S., 2004, MNRAS, 350, 1049
Glikman E., Helfand D. J., White R. L., 2006, ApJ, 640, 579
González Delgado R. M., Heckman T., Leitherer C., 2001, ApJ, 546, 845
Goto T., 2006, MNRAS, 371, 769
Haas M., et al., 2003, A&A, 402, 87
Haba Y., Terashima Y., Kunieda H., Ohsuga K., 2008, PASJ, 60, 487
Hamann F., Ferland G., 1993, ApJ, 418, 11
Hao H., et al., 2010, ApJL, 724, L59
Häring N., Rix H.-W., 2004, ApJL, 604, L89
Hasinger G., 2008, A&A, 490, 905
Hayashida K., 2000, New Astron. Rev., 44, 419
Heckman T. M., Blitz L., Wilson A. S., Armus L., Miley, G. K., 1989, ApJ, 342, 735
Hönig S. F., Beckert T., Ohnaka K., Weigelt G., 2006, A&A, 452, 459
Houck J. C., Chevalier R. A., 1991, ApJ, 376, 234
Hunt L. K., Malkan M. A., Salvati M., Mandolesi N., Palazzi E., Wade R., 1997, ApJS, 108, 229
Jiang L., et al., 2010, Nature, 464, 380
Jiang L., et al., 2006, AJ, 131, 2788
Juarez Y., Maiolino R., Mujica R., Pedani M., Marinoni S., Nagao T., Marconi A., Oliva, E., 2009, A&A, 494, L25
Kaspi S., Smith P. S., Netzer H., Maoz D., Jannuzi B. T., Giveon U., 2000, ApJ, 533, 631
Kato S., Fukue J., Mineshige S., 1998, Black-Hole Accretion discs (Kyoto: Kyoto Univ. Press)
Kato S., Fukue J., Mineshige S., 2008, Black-Hole Accretion discs — Towards a New Paradigm — (Kyoto: Kyoto Univ. Press)
Kawakatu N., Wada K., 2008, ApJ, 681, 73
Kawakatu N., Wada K., 2009, ApJ, 706, 676
Kawaguchi T., Aoki K., Ohta K., Collin S., 2004, A&A, 420, L23
Kawaguchi T., Mori M., 2010, ApJL, 724, L183
Kawanaka N., Kato Y., Mineshige S., 2008, PASJ, 60, 399
King A., 2003, ApJ, 596, L27
Kollmeier J. A., et al., 2006, ApJ, 706, 676
Kormendy J., Richstone D., 1995, ARA&A, 33, 581
Krolik J. H., Begelman M. C., 1988, ApJ, 329, 702
Kubota A., Done C., 2004, MNRAS, 353, 980
Lamastra A., Bianchi S., Matt G., Perola G. C., Barcons X., Carrera F. J., 2009, A&A, 504, 73
Laor A., Draine B. T., 1993, ApJ, 402, 441
Leighly K. M., 1999, ApJS, 125, 297
Maiolino R., Ruiz M., Rieke G. H., Papadopoulos P., 1997, ApJ, 485, 552
Maiolino R., Shemmer O., Imanishi M., Netzer H., Oliva E., Lutz D., Sturm E., 2007, A&A, 468, 979
Malkan M. A., Gorjian V., Tam, R., 1998, ApJS, 117, 25
Marconi A., Hunt L. K., 2003, ApJ, 589, L21
Mathur S., 2000, MNRAS, 314, L17
Matsuoka K., et al., 2009, A&A, 503, 721
McLure R. J., Dunlop, J. S., 2004, MNRAS, 352, 1390
Mineshige S., Kawaguchi T., Takeuchi M., Hayashida K., 2000, PASJ, 52, 499
Minezaki T., Yoshii Y., Kobayashi Y., Enya K., Suganuma M., Tomita H., Aoki T., Peterson,B. A., 2004, ApJ, 600, L35
Miyoshi M., Moran J., Herrnstein J., Greenhill L., Nakai N., Diamond P., Inoue M., 1995, Nature, 373, 127
Mor R., Netzer H., Elitzur M., 2009, ApJ, 705, 298
Mushotzky R. F., Winter L. M., McIntosh D. H., Tueller J., 2008, ApJL, 684, L65
Nagao T., Maiolino R., Marconi A., 2006a, A&A, 447, 863
Nagao T., Maiolino R., Marconi A., 2006b, A&A, 447, 157
Nayakshin S., Kallman T. R., 2001, ApJ, 546, 406
Nenkova M., Sirocky M. M., Nikutta R., Ivezić Ž., Elitzur M., 2008, ApJ, 685, 160
Netzer H., Laor A., 1993, ApJ, 404, L51
Nenkova M., Ivezić Ž., Elitzur M., 2002, ApJ, 570, L9
Netzer H., Shemmer O., Maiolino R., Oliva E., Croom S., Corbett E., di Fabrizio L., 2004, ApJ, 614, 558
Noguchi K., Terashima Y., Ishino Y., Hashimoto Y., Koss M., Ueda Y., Awaki, H., 2010, ApJ, 711, 144
Ohsuga K., Umemura M., 1999, ApJL, 521, L13

Ohsuga K., Umemura M., 2001, ApJ, 559, 157
Ohsuga K., et al., 2005, ApJ, 628, 368
Ohsuga K., 2007, ApJ, 659, 205
Ohsuga K., Mineshige S., 2007, ApJ, 670, 1283
Ohsuga K., Mineshige S., Mori M., Kato Y., 2009, PASJ, 61, L7
Osterbrock D. E., Pogge R. W., 1985, ApJ, 297, 166
Otani C., Kii T., Miya K., 1996 in Röntgenstrahlung from the Universe (MPE Report 263), ed. H. U. Zimmermann, J. E. Trümper, H. Yorke (Garching, MPE Press), 491
Pentericci L., Fan X., Rix H.-W., et al., 2002, AJ, 123, 2151
Perez-Olea D. E., Colina L., 1996, ApJ, 468, 191
Pier E. A., Voit G. M., 1995, ApJ, 450, 628
Pier E. A., Krolik J. H., 1992, ApJL, 399, L23
Pogge R. W., 2000, New Astron. Rev., 44, 381
Pounds K. A., Done, C., Osborne, J., 1995, MNRAS 277, L5
Reynolds C. S., Begelman M. C., 1997, ApJ, 488, 109
Rieke G. H., 1978, ApJ, 226, 550
Rodríguez-Ardila A., Pastoriza M. G., Donzelli C. J., 2000, ApJS, 126, 63
Rodríguez-Ardila A., Mazzalay X., 2006, MNRAS, 367, L57
Ryan C. J., De Robertis M. M., Virani S., Laor A., Dawson P. C., 2007, ApJ, 654, 799
Sani E., Lutz D., Risaliti G., Netzer H., Gallo L. C., Trakhtenbrot B., Sturm E., Boller T., 2010, MNRAS, 403, 1246
Schartmann M., Meisenheimer K., Klahr H., Camenzind M., Wolf S., Henning, T., 2009, MNRAS, 393, 759
Schmitt H. R., Storchi-Bergmann T., Cid Fernandes R., 1999, MNRAS, 303, 173
Schweitzer M., et al., 2008, ApJ, 679, 101
Shakura N. I., Syunyaev R. A., 1973, A&A, 24, 337
Shapiro S. L., 2005, ApJ, 620, 59
Shemmer O., et al., 2006, ApJ, 644, 86
Shen Y., Greene J. E., Strauss M. A., Richards G. T., Schneider D. P., 2008, ApJ, 680, 169
Silk J., Rees M. J., 1998, A&A, 331, L1
Storchi-Bergmann T., Raimann D., Bica E. L. D., Fraquelli H. A., 2000, ApJ, 544, 747
Suganuma M., et al., 2006, ApJ, 639, 46
Thompson T. A., Quataert E., Murray N., 2005, ApJ, 630, 167
Ueda Y., Akiyama M., Ohta K., Miyaji T., 2003, ApJ, 598, 886
Volonteri M., Rees M. J., 2005, ApJ, 633, 624
Wada K., Norman C. A., 2002, ApJL, 566, L21
Wada K., Tomisaka K., 2005, ApJ, 619, 93
Wada K., Papadopoulos P. P., Spaans M., 2009, ApJ, 702, 63
Watabe Y., Umemura M., 2005, ApJ, 618, 649
Watarai K.-Y, Fukue J., 1999, PASJ, 51, 725
Watarai K.-Y, Fukue J., Takeuchi M., Mineshige S., 2000, PASJ, 52, 133
Watarai K.-Y., Ohsuga K., Takahashi R., Fukue, J., 2005, PASJ, 57, 513
Willott C. J., et al., 2010, AJ, 140, 546
Willott C. J., et al., 2007, AJ, 134, 2435
Yamada T., et al., 2009, ApJ, 699, 1354

This paper has been typeset from a TEX/ LATEX file prepared by the author.